Seizure 2003; **12:** 448–455
doi:10.1016/S1059–1311(03)00002-5

Magnetoencephalographic analysis of bilaterally synchronous discharges in benign rolandic epilepsy of childhood

YUNG-YANG LIN[†,‡,¶], KAI-PING CHANG[§,¶], JEN-CHUEN HSIEH[†,¶,‖], TZU-CHEN YEH[†,¶], HSIANG-Yu Yu[‡,¶], SHANG-YEONG KWAN[‡,¶], DER-JEN YEN[‡,¶], CHUN-HING YIU[‡,¶] & RIITTA HARI[††]

[†]*Integrated Brain Research Unit, Department of Medical Research and Education;* [‡]*Department of Neurology, Neurological Institute;* [§]*Department of Pediatrics, Taipei Veterans General Hospital, No. 201, Sector 2, Shih-Pai Road, Taipei 11217, Taiwan, ROC;* [¶]*School of Medicine;* [‖]*School of Life Science, National Yang-Ming University, Taipei 112, Taiwan, ROC;* [††]*Brain Research Unit, Low Temperature Laboratory, Helsinki University of Technology, FIN-02015 HUT Espoo, Finland*

Correspondence to: Dr Yung-Yang Lin, Integrated Brain Research Unit, Department of Medical Research and Education, Taipei Veterans General Hospital, No. 201, Sector 2, Shih-Pai Road, Taipei 11217, Taiwan, ROC.
E-mail: yylin@vghtpe.gov.tw

The purpose of this study was to examine the spatial and temporal relationship between bilateral foci of bilaterally synchronous discharges in benign rolandic epilepsy of childhood (BREC) using a whole-scalp neuromagnetometer. We simultaneously recorded interictal magnetoencephalographic (MEG) and electroencephalographic (EEG) signals in six children with BREC. Interictal spikes were classified into three groups: bilaterally synchronous discharges (BSDs), unilateral discharges on right side (UD-R), and unilateral discharges on left side (UD-L). We used equivalent current dipole (ECD) modelling to analyse the cortical sources of interictal spikes. Both BSDs and UDs were found in Patients 1–4, whereas only UDs were identified in Patients 5 and 6. The ECDs of interictal spikes were located in rolandic regions, 10–20 mm anterior and lateral to hand somatosensory cortices. Multi-dipole analysis of BSDs showed two ECDs in homotopic motor areas of the hemispheres. During BSDs, the right-sided activation preceded the left-sided activation by 15–21 milliseconds in Patients 1 and 2. In Patients 3 and 4, the activation occurred 17–20 milliseconds earlier in the left than the right hemisphere. Within the same hemisphere, the sources of BSDs and UDs were located in similar areas. In conclusion, our results imply the cortical epileptogenicity in bilateral perirolandic areas in BREC. The sequential activation during BSDs in both hemispheres suggest the existence of synaptic connections, possibly via the corpus callosum, between bilateral irritative foci.

Key words: magnetoencephalography; benign rolandic epilepsy of childhood; source localisation; bilaterally synchronous discharges; interictal spikes.

INTRODUCTION

Benign rolandic epilepsy of childhood (BREC) is a common primary partial epilepsy syndrome. The clinical characteristics are onset between 2 and 13 years, a normal neurodevelopment profile, and nocturnal or diurnal brief seizures with stereotyped motor and sensory behaviours. The prognosis is excellent, with a complete recovery of clinical symptoms by the age of 15 years[1–7]. The interictal electroencephalography (EEG) shows normal background activity and scalp-negative spikes, maximal in amplitude in the centrotemporal region[6, 8–12].

Interictal EEG spikes of patients with BREC have been analysed with an emphasis on voltage gradients[1], scalp topography[10, 13], and dipole localisations[11, 14, 15]. These studies have suggested that the spikes are generated in rolandic region. In more recent magnetoencephalography (MEG) studies, the generators of the rolandic discharges (RDs) have been identified in the rolandic region near to the somatosensory cortex; consequently a generation mechanism similar

to that for the middle-latency somatosensory evoked responses has been proposed[12, 16–18]. However, the neuronal generation mechanisms of RDs remain still incompletely known.

The RDs may be unilateral or bilateral[2, 3], and even bilaterally synchronous paroxysms have been observed[2]. Compared with instruments with incomplete head coverage, whole-scalp neuromagnetometers make feasible investigations on bilateral neuronal activation. Using a whole-scalp MEG system, we simultaneously recorded EEG and MEG signals from patients with BREC, and applied equivalent current dipole (ECD) modelling to analyse the unilateral (UDs) and bilaterally synchronous discharges (BSDs). Special attention was paid on the spatiotemporal characteristics of BSDs. We also compared the source locations of UDs with those of BSDs in the same hemisphere.

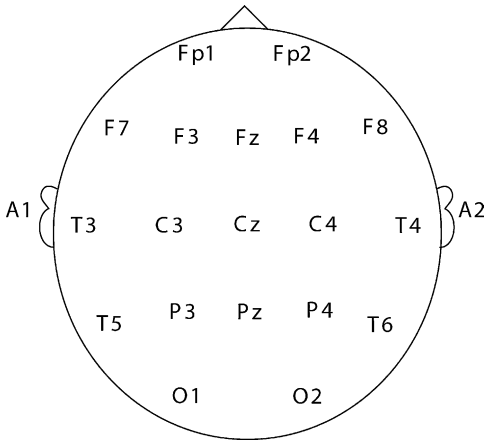

Fig. 1: Placement of scalp EEG electrodes according to the International 10–20 System.

MATERIALS AND METHODS

Patients

We studied six children (1 boy, 5 girls; ages 8–12 years) who were diagnosed as benign rolandic epilepsy according to infrequent motor seizures, normal neurodevelopment, and evidence of centrotemporal spikes on scalp EEG recordings. Table 1 shows the clinical information. The patients had no neurological deficits. Patients 1 and 2 had nocturnal generalised convulsions. Patients 3 and 4 had nocturnal clonic convulsions of right limbs; Patient 5 suffered from occasional convulsions of left limbs. Nocturnal contractions of facial muscles with salivation were noted in Patient 6. Carbamazepine (100 mg, twice a day) was given to Patient 3, whereas the other patients did not use antiepileptic drugs.

MEG recordings

MEG recordings were conducted in a magnetically shielded room with a whole-scalp 306-channel neuromagnetometer (Vectorview^{TM}, 4-D Neuroimaging, San Diego, USA) that comprises 102 identical triple sensor elements. Each sensor element consists of two orthogonal planar gradiometers and one magnetometer coupled to 3 SQUIDs (superconducting quantum interference devices) and thus provides three independent measures of the magnetic fields. During the recordings, the patient was lying comfortably with the head supported against the helmet of the magnetometer. The exact location of the head with respect to the sensors was found by measuring magnetic signals produced by currents led to four head indicator coils, placed at known sites on the scalp. The locations of the coils with respect to anatomical landmarks on the head were determined with a three-dimensional (3-D) digitiser to allow alignment of the MEG and magnetic resonance (MR) image coordinate systems[19]. MR images of the patient's brain were acquired with a 3-T Brucker Medspec300 scanner (Germany).

Simultaneously with the MEG measurements, scalp EEG was recorded according to the International 10–20 System (Fig. 1). MEG and EEG signals were recorded for 3–4 minutes epochs, and in total, 10 recording epochs were obtained for each individual. Head position was measured immediately prior to each recording session.

Table 1: Summary of clinical data.

Patient no.	Sex/age (y)	Onset age (y)	Handedness	Seizure type	Seizures since onset
1	F/12	5	Right	GCS	3 seizures
2	M/8	6	Right	GCS	3 seizures
3	F/9	6	Right	PMS, RL	6 seizures
4	F/9	8	Left	PMS, RL	4 seizures
5	F/9	8	Right	PMS, LL	3 seizures
6	F/8	6	Right	FC, Saliv	4 seizures

GTCS, generalized convulsive seizure; PMS, partial motor seizure; RL, right limbs; LL, left limbs; FC, facial contraction; Saliv, salivation.

Somatosensory evoked fields (SEFs) were recorded to obtain functional landmarks. The right and left median nerves were stimulated with 0.2 milliseconds constant-current pulses once every 1 second. The recording passbands and signal digitisation rates were 0.03–200 and 600 Hz, respectively.

Classification of spikes

Interictal spikes were visually checked on both EEG and MEG channels. Identified spikes were collected and classified into three groups: unilateral rolandic discharges (UD) in the left hemisphere (UD-L), UD in the right hemisphere (UD-R), and BSDs. BSDs were defined as those bilaterally simultaneous spikes with side-to-side time lag of main peaks less than 50 milliseconds.

Source modelling

ECD model was used to estimate the source locations of spontaneous spikes. The source analysis was based on MEG signals recorded by the 204 gradiometers. Epochs of 400–500 milliseconds duration, with clear interictal spikes, were visually selected for further analysis. During these time windows (from the beginning of the main spike deflection to its return to the baseline level) the magnetic field patterns were first visually surveyed in 2 milliseconds steps to create the initial guess of the number of active sources within that time period and to estimate the stability of the dipolar magnetic field pattern. The ECDs, best describing the measured data, were found by a least-squares search using subsets of 40–60 channels around the maximum signals.

To evaluate the validity of the dipole model, we compared the measured signals with responses predicted by the model. If signals of some brain region were left inadequately explained by the model, the data were re-evaluated for more accurate estimation of the generators. This approach, explained previously in detail[19], has been successfully applied in previous MEG studies[19–21].

In the present study, one ECD could explain most field patterns of unilateral spikes. For BSDs, two ECDs were applied with one dipole located in each hemisphere. For SEFs, single ECD, identified during the P35m deflection, was used to explain the cortical responses to contralateral median nerve stimulation. These calculations resulted in the 3-D locations, orientations, and strengths of the ECDs in a spherical conductor model, which was based on the patient's own MR images.

Data analysis and statistics

After artifact rejection, 10–15 consecutive spikes of each group were identified in each patient. We localized the sources of these spikes and then measured the time difference between bilateral sources. Statistical significance was tested by Student's paired two-tailed *t*-test.

RESULTS

Table 1 summarises the clinical information of the six patients. From simultaneous MEG and EEG recordings, UD-R, UD-L, and BSD were found in Patients 1–3, UD-L and BSD in Patient 4, UD-R and UD-L in Patient 5, and UD-L in Patient 6. Because BSDs were identified in Patients 1–4, further results in this paper were based on data from them. Fig. 2 shows interictal spikes in simultaneous EEG and MEG recordings of the 4 patients with BSDs. Spike discharges occurred either on one side only (UD-R or UD-L) or synchronously in both hemispheres (BSD). In EEG, the largest phase-reversal negativity was identified on central electrodes. Spikes were clearly seen also on MEG channels selected from the central head regions. In the present study, most spikes ($98.1 \pm 0.6\%$; mean $\pm$ SEM) were simultaneously seen in both EEG and MEG channels; few were exclusively seen in either EEG ($0.3 \pm 0.2\%$) or MEG ($1.6 \pm 0.6\%$) only.

Fig. 3 shows the topographic distributions of BSD signals in MEG from Patient 1 (left half) and Patient 3 (right half). Clear spike signals are present in the centrotemporal regions of both hemispheres. The enlarged signals in inserts show the close resemblance of the measured signals (solid lines) to those predicted by a two-dipole model (dashed lines), with one current dipole in each hemisphere (also see Fig. 4).

Fig. 4 shows the dipole locations and waveforms of the bilateral spikes from Patients 1 (left half) and 3 (right half). The activation of the right-hemisphere source leads the left-hemisphere activation by 18 milliseconds in Patient 1 and by 14 milliseconds in Patient 3. In these subjects, as well in the 2 others, the sources of spikes (white dots) are located homotopically in bilateral rolandic regions, 10–20 mm (see Table 2) anterior and 2–10 mm lateral to the sources of the P35m somatosensory responses (black dots) to median nerve stimulation. These spikes therefore originate most likely in the primary motor cortex.

In each patient, 12 paroxysms of UD-L, UD-R, and BSD subgroups with no contamination by visible artifacts were selected for further analysis and statistics. Table 2 shows the mean locations and strengths of

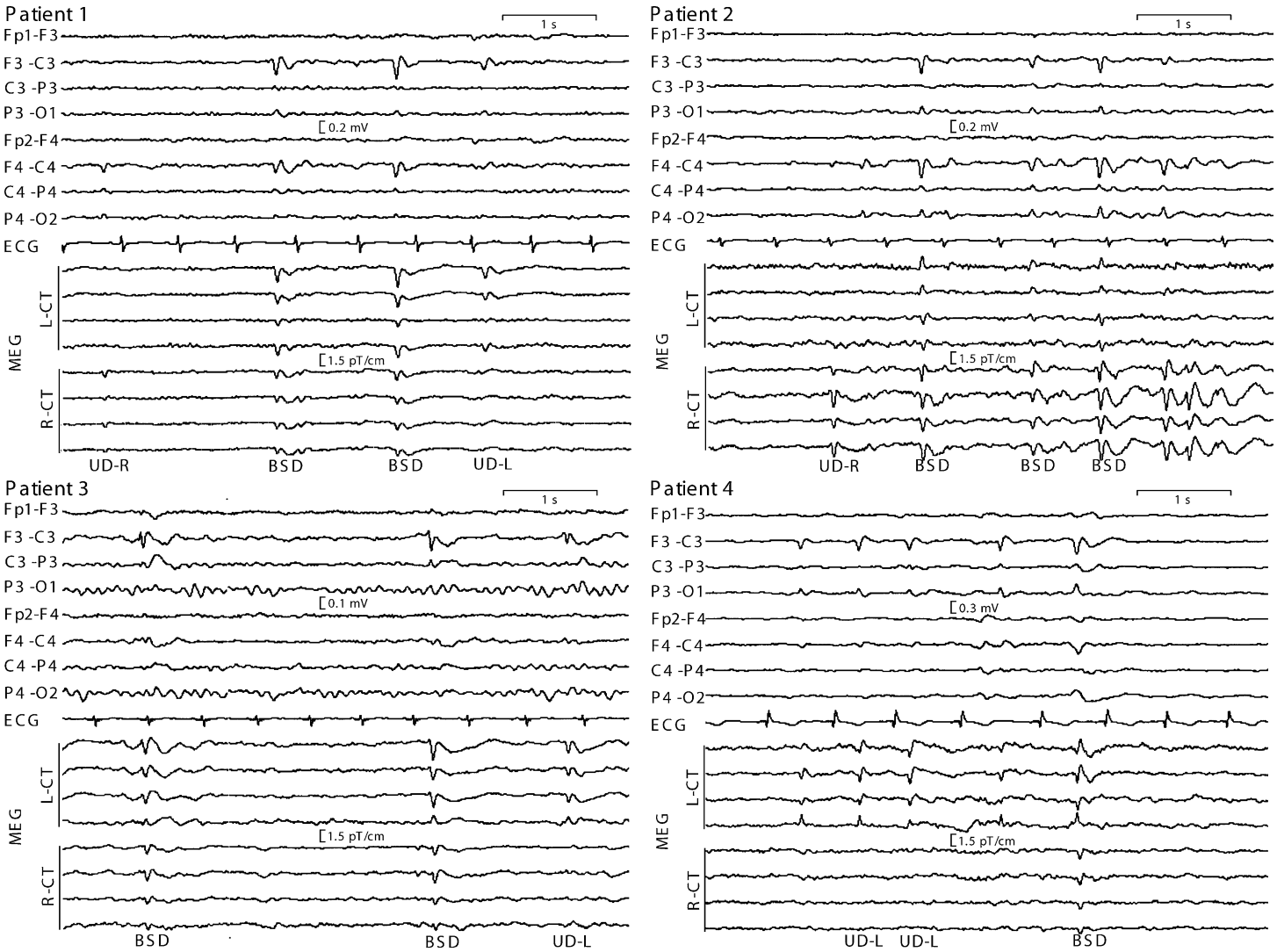

Fig. 2: Simultaneous MEG and EEG signals in Patients 1–4. Interictal spike discharges, maximal in central MEG and EEG channels, are present either bilaterally synchronously (BSD) or unilaterally (UD-R, UD-L). The signals were low-pass filtered at 40 Hz. CT, centrotemporal; ECG, electrocardiogram; R, right side; L, left side.

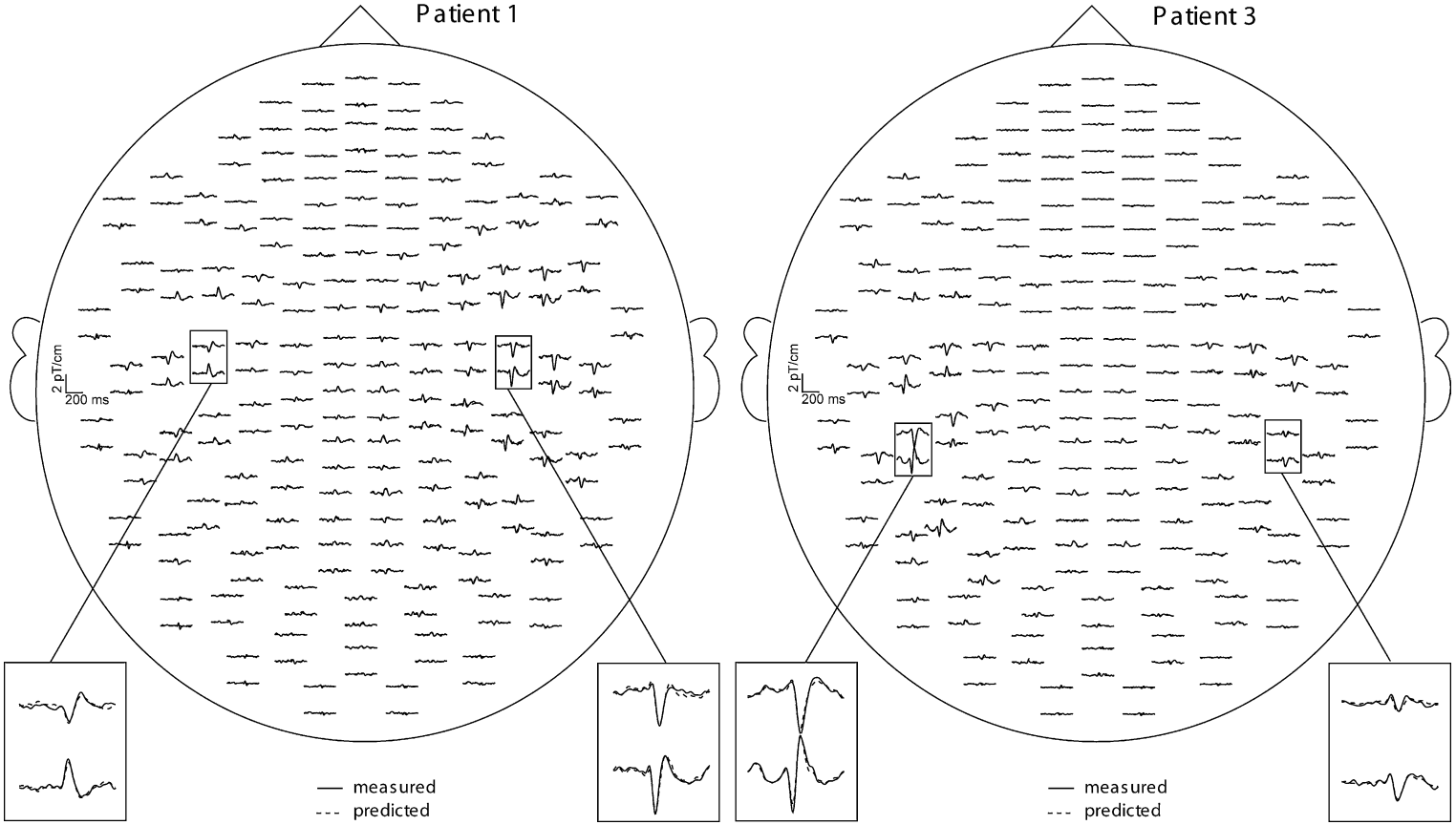

Fig. 3: Distribution of bilateral rolandic discharges in Patient 1 (left) and Patient 3 (right). The head is viewed from the top, and each response pair illustrates signals recorded by the two orthogonal gradiometers of a signal sensor unit. The inserts show enlarged responses from the framed areas with the measured signals superimposed by the waveforms (dashed lines) predicted by the two equivalent current dipoles, one in each hemisphere.

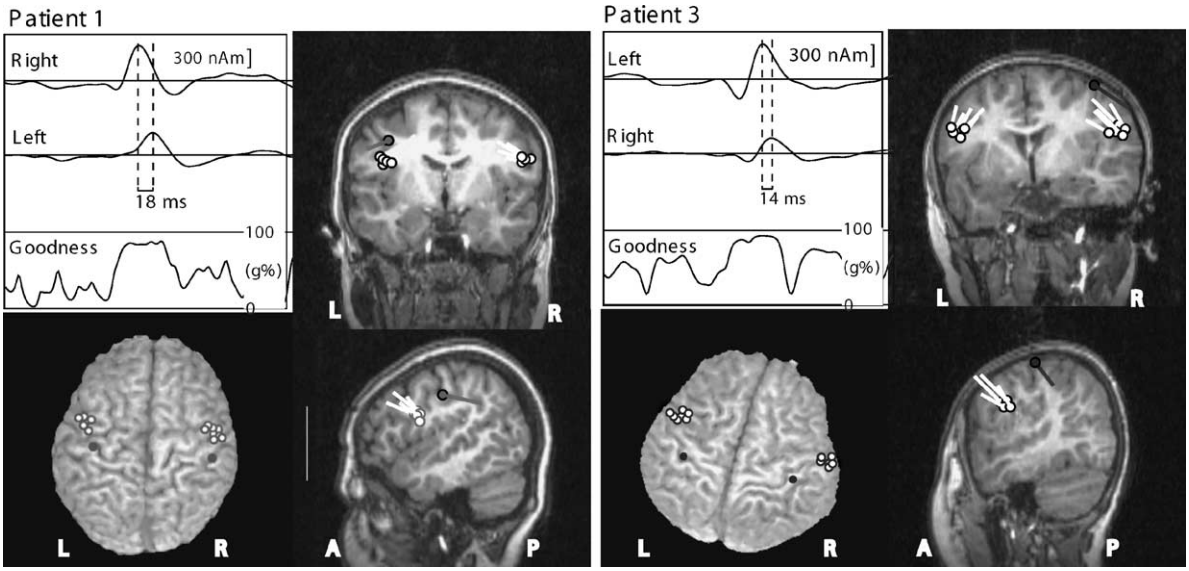

Fig. 4: Source waveforms (left upper part in each patient's panel) of the bilaterally synchronous discharges (BSDs) as a function of time displayed in Fig. 3 from Patients 1 and 3. The interval between dashed lines indicates the peak time difference between bilateral sources. Source locations of 5–7 BSDs (white dots) are superimposed on patient's own MRI slices (right part in each patient's panel) and 3-D rendering of the brain (left lower part in each patient's panel). Sources of somatosensory cortical responses (P35m, black dots) to median nerve stimulation are also indicated for anatomical landmarks.

spikes in each patient in comparison with P35m somatosensory responses to electric stimulation. In the same hemisphere, the sources of UDs were situated in the same region with those of BSDs.

Table 3 summarises the number and types of rolandic spikes identified: BSD, UD-L, and UD-R in Patients 1, 2, and 3; BSD and UD-L in Patient 4.

Table 2: Mean (±SEM) source locations and strengths of 12 consecutive spikes.

Patient no.	Spike	*x* (mm)	*y* (mm)	*z* (mm)	Strength (nAm)
1	UD-L	−42.0 ± 1.0	22.4 ± 0.8	74.8 ± 0.9	524 ± 52
	BSD-L	−44.5 ± 1.7	21.9 ± 1.2	75.2 ± 1.0	403 ± 74
	UD-R	51.4 ± 1.2	26.2 ± 1.3	73.1 ± 1.2	369 ± 41
	BSD-R	56.7 ± 1.5	25.3 ± 1.6	68.1 ± 3.5	258 ± 43
	P35m-L	−35.2	10.4	89.6	43.6
	P35m-R	44.5	12.6	91.2	38.4
2	UD-L	−50.4 ± 1.1	17.7 ± 1.0	62.0 ± 1.1	231 ± 21
	BSD-L	−50.1 ± 1.1	17.6 ± 0.6	64.0 ± 1.0	252 ± 30
	UD-R	64.6 ± 1.0	17.1 ± 0.6	56.0 ± 1.5	131 ± 7
	BSD-R	64.7 ± 0.9	14.3 ± 0.6	52.3 ± 1.0	154 ± 10
	P35m-L	−42.9	8.6	84.5	49.4
	P35m-R	57.8	10.4	87.1	42.7
3	UD-L	−45.6 ± 2.8	20.7 ± 3.0	59.7 ± 2.7	404 ± 32
	BSD-L	−39.7 ± 3.4	15.8 ± 3.2	64.4 ± 2.7	559 ± 67
	UD-R	52.4 ± 1.2	16.6 ± 0.7	58.5 ± 0.8	321 ± 18
	BSD-R	46.3 ± 2.8	18.1 ± 2.1	64.2 ± 3.1	544 ± 96
	P35m-L	−34.2	−0.6	92.7	23.8
	P35m-R	45.0	5.1	89.0	25.6
4	UD-L	−42.8 ± 1.9	20.5 ± 2.2	79.3 ± 2.8	489 ± 74
	BSD-L	−43.7 ± 1.2	20.1 ± 1.5	82.8 ± 1.4	362 ± 38
	BSD-R	43.1 ± 3.8	15.8 ± 3.3	75.2 ± 5.9	297 ± 94
	P35m-L	−41.0	8.0	91.7	33.7
	P35m-R	40.2	10.6	100.6	38.2

The source locations of the P35m somatosensory evoked responses to median nerve stimulation were also shown. The positive *x*-, *y*-, and *z*-axes go towards the right preauricular point, the nasion, and the vertex, respectively. UD-L, source of unilateral rolandic discharges (UD) in left hemisphere; UD-R, source of right hemispheric UD; BSD-L, left source of bilaterally synchronous rolandic discharges (BSD); BSD-R, right source of BSD.

Table 3: Number and type of spikes and leading side (LS) of bilaterally synchronous rolandic discharges (BSD).

Patient no.	Total spikes	BSD	UD-L	UD-R	LS of BSD	Time lag in BSD (milliseconds)
1	144	18 (13%)	42 (29%)	84 (58%)	R	15.5 ± 1.7
2	188	48 (26%)	19 (10%)	121 (64%)	R	21.4 ± 2.1
3	96	43 (45%)	21 (22%)	32 (33%)	L	16.4 ± 1.9
4	222	68 (31%)	154 (69%)	0 (0%)	L	20.4 ± 1.7

UD-L, unilateral rolandic discharges in left hemisphere; UD-R, unilateral rolandic discharges in right hemisphere.

The right-hemisphere source (BSD-R) led the BSDs in Patients 1 and 2, whereas the left-hemisphere source (BSD-L) led the BSDs in Patients 3 and 4. The time difference between bilateral foci of BSD was 15–21 milliseconds.

DISCUSSION

The results of this study show that bilateral homotopic irritative foci are commonly seen in patients with BREC. In line with previous EEG[11, 15] and MEG source analyses[12, 16, 18], our data suggest the precentral locations of rolandic discharges. Most spikes were simultaneously seen on both EEG and MEG, implying that the cortical intracellular currents for most rolandic spikes appear as tangential dipoles. However, to our knowledge, no previous MEG study has analyzed the temporal and spatial characteristics of bilaterally synchronous spikes in BREC.

Our whole-scalp MEG recordings showed prominent spikes in the rolandic areas bilaterally (Fig. 3). Since the planar gradiometers detect the largest signals just above a local active brain area, the distribution patterns of BSD already indicated the existence of two active brain areas. Multi-dipole analysis of BSDs resulted in two ECDs, one in the right and the other in the left motor cortex. The consistent time difference (15–21 milliseconds) between the foci implies the existence of synaptic connections between bilateral perirolandic areas.

BSDs were identified in 4 (67%) out of the 6 patients with BREC, in agreement with Lombroso's[1] observation of a high number of bilateral rolandic spikes. Using MEG source modelling, we found the same source locations for both BSD and UD in the same hemisphere (Table 2), indicating the presence of common or close cortical generators for both UD and BSD. The consistent leading side for BSD in each individual (right side in Patients 1 and 2; left side in Patients 3 and 4) suggested the presence of an earlier activation in one hemisphere during paroxysms of individual BSD with later activation in the other hemisphere. Clinically, the seizure patterns of patients with BREC may be generalised convulsions or partial seizures. Some authors have suggested the anatomical relation of rolandic spikes to clinical semiology of partial seizures[12, 13, 16, 18]. In our study, the early activation focus of BSD was situated in the left hemisphere in Patients 3 and 4, correlating with their ictal convulsions of right limbs. However, the correlation between the early BSD foci and the clinical semiology cannot be applied in Patients 1 and 2 who suffered from nocturnal generalised convulsions. Further studies in more patients would help to explore the roles of the earlier BSD foci in BREC.

The mechanisms for BSDs have not been well known[22–24]. Forebrain commissures[25–27] and subcortical structures[28–30] have been reported as possible origins for BSDs. The presence of both independent and bi-synchronous irritative foci in our study indicates bilateral cortical excitability in patients with BREC. The ~20 milliseconds time lag between peak activations of bilateral BSDs foci may be more in favor of transcallosal conduction[31], although our study does not exclude the possible involvement of diencephalic and mesencephalic structures in the formation of BSDs[32].

Recent studies have suggested contribution of pericentral areas to the formation of epileptogenicity in BREC[12, 13, 16, 18]. However, the pathogenesis of rolandic epilepsy is still unknown. Genetically-determined unknown factors or some developmental problems have been proposed[16]. The occurrence of bilaterally synchronous spike-and-wave discharges have raised the question of subcortical origin for rolandic epileptic foci[1]. Our present data showed the presence of bilateral cortical excitability with intermittent sequential activation between homologous rolandic areas. BREC appears to be a maturational or developmental abnormality that can affect multiple brain areas without progressive neurophysiological or pathological deteriorations in the vast majority of patients[4]. The sequential activation patterns of our BREC patients probably indicate that rolandic spikes trigger spikes in the contralateral irritative areas.

In kittens, development of thalamocortical projections varies between different cortical lobes and the synaptogenesis proceeds from the deep to the more superficial layer[33]. The maturation failure of rolandic cortices with consequent neuronal hyperexcitability might be related to the formation of irritative foci in BREC. The phenomenon of sequential epileptic foci can be presumed to be the consequence of intrinsic

neural plasticity and the persistent synaptic activation of neuronal populations that are functionally and anatomically related to one another. Further longitudinal studies are warranted for elucidation of the entire pathophysiological process of rolandic epileptic discharges.

ACKNOWLEDGEMENT

We thank Mr Chih-Che Chou and Mr Chou-Ming Cheng for technical assistance in the acquisition of MR images. This study was supported in part by research grants VGH-92-386-(3), VGH-90-370 and VGH-91-329 from Taipei Veterans General Hospital and NSC-91-2314-B-075-056 from the National Science Council, Taipei, Taiwan.

REFERENCES

1. Lombroso, C. T. Sylvian seizures and midtemporal spike foci in children. *Archives of Neurology* 1967; **17**: 52–59.
2. Blom, S., Heijbel, J. and Bergfors, P. G. Benign epilepsy of children with centro-temporal EEG foci. Prevalence and follow-up study of 40 patients. *Epilepsia* 1972; **13**: 609–619.
3. Lerman, P. and Kivity, S. Benign focal epilepsy of childhood. A follow-up study of 100 recovered patients. *Archives of Neurology* 1975; **32**: 261–264.
4. Lüders, H., Lesser, R. P., Dinner, D. S. and Morris, H. H. Benign focal epilepsy of childhood. In: *Epilepsy: Electroclinical Syndromes* (Eds H. Lüders and R. P. Lesser). London, Springer, 1987: pp. 303–346.
5. Beydoun, A., Garofalo, E. A. and Drury, I. Generalised spike-waves, multiple loci. and clinical course in children with EEG features of benign epilepsy of childhood with centrotemporal spikes. *Epilepsia* 1992; **33**: 1091–1096.
6. Holmes, G. L. Benign focal epilepsies of childhood. *Epilepsia* 1993; **34** (Suppl. 3): S49–S61.
7. Legarda, S. and Jayakar, P. Electroclinical significance of rolandic spikes and dipoles in neurodevelopmentally normal children. *Electroencephalography and Clinical Neurophysiology* 1995; **95**: 257–259.
8. Lischka, A. and Graf, M. Benign rolandic epilepsy of childhood: topographic EEG analysis. *Epilepsy Research Supplement* 1992; **2**: 53–58.
9. Loiseau, P. and Duche, B. Benign rolandic epilepsy. *Advances in Neurology* 1992; **57**: 411–417.
10. Van der Meij, W., Van Huffelen, A. C., Wienecke, G. H. and Williemse, J. Sequential EEG mapping may differentiate “epileptic” from “nonepileptic” rolandic spikes. *Electroencephalography and Clinical Neurophysiology* 1992; **82**: 408–414.
11. Baumgartner, C., Graf, M., Doppelbauer, A. *et al.* The functional organization of interictal spike complex in benign rolandic epilepsy. *Epilepsia* 1996; **37**: 1164–1174.
12. Minami, T., Gondo, K., Yamamoto, T., Yanai, S., Tasaki, K. and Ueda, K. Magnetoencephalographic analysis of rolandic discharges in benign childhood epilepsy. *Annals of Neurology* 1996; **39**: 326–334.
13. Gregory, D. L. and Wong, P. K. Topographical analysis of the centrotemporal discharges in benign rolandic epilepsy of childhood. *Epilepsia* 1984; **25**: 705–711.
14. Weinberg, H., Wong, P. K., Crisp, D., Johnson, B. and Cheyne, D. Use of multiple dipole analysis for the classification of benign rolandic epilepsy. *Brain Topography* 1990; **3**: 183–190.
15. Wong, P. K. Source modelling of the rolandic focus. *Brain Topography* 1991; **4**: 105–112.
16. Kubota, M., Oka, A., Kin, S. and Sakakihara, Y. Generators of rolandic discharges identified by magnetoencephalography. *Electroencephalography and Clinical Neurophysiology Supplement* 1996; **47**: 393–401.
17. Kubota, M., Takeshita, K., Sakakihara, Y. and Yanagisawa, M. Magnetoencephalographic study of giant somatosensory evoked responses in patients with rolandic epilepsy. *Journal of Child Neurology* 2000; **15**: 370–379.
18. Kamada, K., Moller, M., Saguer, M. *et al.* Localisation analysis of neuronal activities in benign rolandic epilepsy using magnetoencephalography. *Journal of Neurological Science* 1998; **154**: 164–172.
19. Hämäläinen, M., Hari, R., Ilmoniemi, R. J., Knuutila, J. and Lounasmaa, O. V. Magnetoencephalography: theory, instrumentation, and applications to noninvasive studies of the working human brain. *Review of Modern Physics* 1993; **65**: 413–497.
20. Lin, Y. Y., Simões, C., Forss, N. and Hari, R. Differential effects of muscle contraction from various body parts on neuromagnetic somatosensory responses. *Neuroimage* 2000; **11**: 334–340.
21. Lin, Y. Y., Wu, Z. A., Hsieh, J. C., et al. Magnetoencephalographic study of rhythmic mid-temporal discharges in nonepileptic and epileptic patients. *Seizure* 2003 (in press).
22. Tukel, K. and Jasper, H. The electroencephalogram in parasagittal lesions. *Electroencephalography and Clinical Neurophysiology* 1952; **4**: 481–494.
23. Ogden, T. E., Aird, R. B. and Garoutte, B. C. The nature of bilateral and synchronous cerebral spiking. *Acta Psychiatry Neurology of Scandinavia* 1956; **31**: 273–284.
24. Marcus, E. M., Watson, C. W. and Simon, S. A. An experimental model of some varieties of petit mal epilepsy: electrical behavior correlations of acute bilateral epileptogenic foci in cerebral cortex. *Epilepsia* 1968; **9**: 233–248.
25. Walker, A. E. and Udvarhelyi, G. B. The generalization of a seizure. *Journal of Nervous and Mental Disease* 1965; **140**: 252–271.
26. Marcus, E. M. and Watson, C. W. Bilateral synchronous spike wave electrographic patterns in the cat. *Archives of Neurology* 1966; **14**: 601–610.
27. Musgrave, J. and Gloor, P. The role of the corpus callosum in bilateral interhemispheric synchrony of spike and wave discharge in feline generalised penicillin epilepsy. *Epilepsia* 1980; **21**: 369–378.
28. Rutledge, L. T. and Kennedy, T. T. Extracallosal delayed responses to cortical stimulation in chloralosed cat. *Journal of Neurophysiology* 1960; **23**: 188–196.
29. Mattson, R. H. and Bickford, R. G. Firing patterns of strychnine spikes in the cortex of the cat. *Electroencephalography and Clinical Neurophysiology* 1961; **13**: 144–145.
30. Kopeloff, N., Kennard, M. A., Pacella, B. L., Kopeloff, L. M. and Chusid, J. G. Section of the corpus callosum in experimental epilepsy in the monkey. *Archives of Neurology and Psychiatry* 1950; **63**: 719–727.
31. Hari, R., Ahonen, A., Forss, N. *et al.* Parietal epileptic mirror focus detected with a whole-head neuromagnetometer. *NeuroReport* 1993; **5**: 45–48.
32. Spencer, S. S., Spencer, D. D., Williamson, P. D. and Mattson, R. H. Effects of corpus callosum section on secondary bilaterally synchronous interictal EEG discharges. *Neurology* 1985; **35**: 1689–1694.
33. Kawaguchi, S., Samejima, A. and Yamamoto, T. Postnatal development of the cerebello-cerebral projection in kittens. *Journal of Physiology* 1983; **343**: 215–232.